ISSN 1027-4510, Journal of Surface Investigation. X-ray, Synchrotron and Neutron Techniques, 2015, Vol. 9, No. 6, pp. 1287–1292. © Pleiades Publishing, Ltd., 2015.
Original Russian Text © P.Yu. Grigorev, D.A. Terentyev, A.V. Bakaev, E.E. Zhurkin, 2015, published in Poverkhnost'. Rentgenovskie, Sinkhrotronnye i Neitronnye Issledovaniya, 2015, No. 12, pp. 84–90.

Interaction of Hydrogen with Dislocations and Grain Boundaries in Tungsten

P. Yu. Grigorev[a, b], D. A. Terentyev[b], A. V. Bakaev[a, b], and E. E. Zhurkin[a]

[a] *St. Petersburg Polytechnic University, St. Petersburg, 195251 Russia*
e-mail: ezhurkin@phmf.spbstu.ru
[b] *Belgian Nuclear Research Center (SCK · CEN), 2400 Mol, Belgium*

Received March 4, 2015

Abstract—A kinetic model of hydrogen capture and accumulation in tungsten under low-energy bombardment with hydrogen atoms in the "subthreshold" mode is proposed in this paper. Primary defects do not form in the bombarded material in this mode. This model takes into account the physical mechanisms for hydrogen bubble nucleation and growth at dislocations, i.e., the presence of "traps" in the dislocation core and dislocation jog formation due to interstitial tungsten-atom emission during the bubble growth process. Features of the dynamics of bubble growth as a function of the temperature and the hydrogen flux are studied. It is shown that there is a "threshold" temperature that is dependent on the flux of implanted particles and above which the process of hydrogen-bubble formation is suppressed significantly. The obtained estimates of the "threshold" temperature (600–700 K for a flux in the range of 10^{22}–10^{23} m^{-2} s^{-1}) agree with existing published experimental data.

Keywords: tungsten, low-energy implantation, diffusion, hydrogen capture and accumulation, dislocation
DOI: 10.1134/S1027451015060270

INTRODUCTION

At present, tungsten is the main candidate material for the coating of diverter plates at the International Thermonuclear Experimental Reactor (ITER) [1]. This is why a large number of experimental research dedicated to studying the characteristics of tungsten as applied to problems of the ITER are performed. In spite of the fact that W has a series of unique properties (a high melting temperature, a low sputtering coefficient, and high thermal conductivity) required for operation under high-temperature conditions, some issues concerning the use of W in the ITER remain insurmountable. The capture and retention of hydrogen isotopes (HI), in particular, tritium, is one such issue [2], which is caused by problems relating to the safe operation of thermonuclear equipment.

Ion beams or linear plasma generators are usually used in experiments aimed at studying the plasma–material interaction under conditions close to the ITER. In this case, as a rule, the ion energy does not exceed several tens of electronvolts [3–5], which corresponds to a so-called "subthreshold" bombardment mode at which the kinetic energy of impinging plasma ions is insufficient to form stable Frenkel pairs (because the energy of the primary knock-on W atoms turns out to be smaller than the threshold displacement energy). This means that stable primary defects of the crystal lattice do not form under such conditions. Because, unlike helium, the binding energy of two H hydrogen atoms located in W crystals is very small (is on the order of 0.01 eV [6]), nucleation centers ("traps") must be present in the material to form a H cluster; crystal-lattice defects can serve as such centers. In the case of low plasma fluxes (in the "subthreshold" bombardment mode), hydrogen retention is due to gas-atom diffusion in the material and due to their capture at natural defects of the crystal lattice (such as dislocations and polycrystal grain boundaries) in the surface layer. As was established experimentally [3, 7, 8], as the flux increases, hydrogen bubbles and blisters form intensively in tungsten (even if the bombardment conditions correspond to the "subthreshold" mode as before). Analysis of the result of annealing the bombarded samples showed that vacancies make an appreciable contribution to hydrogen capture in addition to natural crystal defects [3]. In a series of experimental papers, the spectra of the HI yield obtained using thermodesorption spectroscopy were interpreted as follows: a significant peak observed at temperatures in the range of 700 to 900 K (depending on the rate of sample heating) corresponds to the yield of hydrogen captured at vacancies, while the hydrogen yield from natural defects gives another peak at a temperature near 450 K [7, 9, 10]. A significant amount of retained hydrogen was found at depths of up to several micrometers [5], where vacancies cannot play a considerable role in HI capture, because their thermal concentration is negligibly small at implantation tem-

peratures (usually smaller than 1000 K). Even if capture is determined by vacancies formed by fluctuations of mechanical-stress and temperature fields in one or another way, growth of the total amount of captured hydrogen with temperature should be expected, because the increase in temperature assists vacancy formation. Experiments using intensive low-energy plasma fluxes and conducted at high temperatures showed the opposite tendency: a noticeable decrease in the effect of hydrogen retention was observed at temperatures above 550 K [8]. The physical explanation of such a temperature effect has not been proposed to date.

Quantitative estimates of the effect of HI retention in materials used in thermonuclear apparatus can be obtained on the basis of various models of hydrogen diffusion in these materials. Such problems can be considered on different spatial levels (scales), namely, from the microscopic (atomic) to the macroscopic. Reviews of the modern state of the theory and numerical simulation were given in [11, 12]. In other works, in particular, in [13, 14], the effects of hydrogen capture and retention in beryllium and different types of graphite were estimated quantitatively using the classical diffusion model. In addition, a similar model was used in [15] to analyze and process thermal desorption spectra (TDS). The authors of series of papers [16–18] proposed a model of one-dimensional hydrogen and monatomic gas diffusion in a plane-parallel plate with first-kind boundary conditions.

Existing models of HI retention in W were based on the assumption that H capture is due to defects created during the bombardment process [19]. Such an approach allows experimental results, in which beams of ions with energies of 5–30 keV/ion are used, to be explained. However, as shown in [20], such a model cannot describe the experimental results obtained under conditions of the "subthreshold" bombardment mode (at ion energies of 1 keV/ion or lower), in particular, the experimentally observed saturation of the amount of retained hydrogen as the total fluence increases. Proceeding from this, it can be concluded that a new model based on alternative mechanisms of H-bubble formation and growth in W must be developed.

In this paper, we consider the kinetics of H accumulation in W (under "subthreshold" bombardment with plasma high fluxes) within the framework of a recently proposed model [21], which takes new mechanisms of HI capture at dislocations into account. The quantum-mechanical (ab initio) calculations carried out in [21] showed that regions of electron-density depletion exist in the screw dislocation core; in this case, H atoms tend to occupy these regions, thus minimizing the system energy. Thus, the dislocation core contains "traps" for H atoms; in this case, each of these "traps" can hold up to seven HI atoms. In addition, the migration barrier for H atoms along the dislocation core (0.2 eV) is significantly lower than in the ideal crystal (0.4 eV) [18], which is indicative of the predominance of one-dimensional HI migration along the dislocation core.

In our model, we suggest that the process of H bubble formation and growth includes the following stages: fast one-dimensional HI migration along the dislocation core, the capture of an interstitial H atom by the dislocation core, the growth of polyatomic H_n clusters leading to the emission of an interstitial W atom (as the H_n cluster reaches a certain critical size n), and the subsequent growth of bubbles because of the emission of interstitial W atoms (with the formation of dislocation jogs and loops). In essence, such a mechanism is similar to the mechanism of gas-bubble growth in metals considered in [23] and related to the emission of interstitial dislocation loops as a certain critical gas pressure is reached inside the bubble. As follows from the results of ab-initio calculations in [21], the formation of dislocation jogs (because of the emission of interstitial W atoms) begins in the case where the number of H atoms in the cluster H_n exceeds the critical value $n = 8$. Thus, the transformation of the cluster from the "subthreshold" state into the state of "stable growth" is determined by the balance between the rate of H-atom capture at the cluster and that of their thermal evaporation.

In this paper, we use the results of quantum-mechanical calculations [21] to develop a model describing the kinetics of HI accumulation in W at the initial state (the mechanism of dislocation jog formation is taken into account) in order to explain the experimentally observed regularities of stable H-bubble formation and growth, depending on bombardment conditions (the plasma flux and temperature). It is important to note that such a model can be used to estimate H capture not only inside grains of polycrystalline W, but also at small-angle grain boundaries, because such boundaries are arrays of a given type of dislocations [24].

SIMULATION PROCEDURE

Kinetic equations describing hydrogen capture at "traps" and the subsequent growth of bubbles was integrated numerically. The steady-state spatial hydrogen distribution in a half-finite W target, whose surface was bombarded with a flux of low-energy hydrogen atoms, was the initial condition for the solution of such equations. To obtain such a distribution, we consider the boundary-value problem corresponding to diffusion under the condition of implantation. In the case of low-energy subthreshold implantation, the hydrogen range R in tungsten is on the order of several nanometers [20]. To establish the steady-state mode, it is necessary for the diffusion hydrogen flux from the target material to be counterbalanced by the

implantation one, which can be expressed using the following relation [7]:

$$F = D\frac{dC}{dx}, \quad (1)$$

where F is the flux of implanted atoms (i.e., the fluence per time unit), D is the diffusion coefficient, C is the hydrogen concentration, and x is the depth measured from the surface.

Since all implanted atoms are at a depth within the limits of several nanometers [20] (i.e., $x \sim R$), it can be assumed that the diffusion hydrogen-atom flux from the material is determined using the maximum hydrogen concentration at the implantation depth (C_R). By replacing the derivative with the finite differences in formula (1), we obtain

$$F = D\frac{(C_S - C_R)}{(X_S - R)}, \quad (2)$$

where C_S is the hydrogen concentration at the target surface, X_S is the surface coordinate (in our case, we set $X_S = 0$), and C_R is the hydrogen concentration at the implantation depth R. If it is assumed that the process of the thermal recombination of hydrogen atoms and their escape from the surface occur instantaneously, then $C_S = 0$ can be set. In such a case, if (2) is taken into account, then C_R can be found:

$$C_R = \frac{FR}{D}, \quad (3)$$

where R is the average hydrogen-atom range in tungsten, F is the flux of implanted atoms, and $D = D_0 \exp\left(-\frac{E_m}{kT}\right)$ is the diffusion coefficient.

We then consider the equation of hydrogen diffusion in the field of traps [23]:

$$\frac{\partial C_\mathrm{H}}{\partial t} = D\frac{d^2C_\mathrm{H}}{dx^2} - k^2 DC_\mathrm{H}, \quad (4)$$

where C_H is the distribution of the hydrogen concentration over depth x and k^2 is the sink intensity (taking hydrogen capture at traps into account). To consider the steady-state problem, we set $\frac{\partial C_\mathrm{H}}{\partial t} = 0$. Under the assumption that traps are dislocations, the sink intensity is defined as $k = \sqrt{\rho}$, where ρ is the dislocation density, which is $\sim 10^{12}$ m^{-2}. As was mentioned above, for low-energy implantation, the H-atom range in W (R) is on the order of several nanometers. At the same time, the experimental profiles of H location (with diffusion taken into account) extend to a depth x of tens of micrometers, i.e., $x \gg R$. Proceeding from the foregoing, when solving Eq. (4), we can conditionally assume that the value of the H concentration at the depth of range (C_R) defined by relation (3) as the boundary condition at the material surface ($x = 0$). Then, using the boundary condition $C(0) = C_R = \frac{FR}{D}$; $C(\infty) = 0$, we can obtain the steady-state solution $C_\mathrm{H}(x)$ (for $x \gg R$) [21]:

$$C_\mathrm{H}(x) = C_R \exp(-x\sqrt{\rho}). \quad (5)$$

In the calculations, we used the value of the H-atom range in W that was equal to several nanometers, and the parameters used to determine the diffusion coefficient were taken from [22] ($D_0 = 4.1 \times 10^{-7}$ m^2/s and $E_m = 0.39$ eV).

The processes of bubble nucleation and time evolution were simulated via solution of the system of kinetic equations whose forms depend on the considered growth stage of hydrogen cluster H_n. We assumed the presence of bubble-nucleation centers related to dislocations in the material; in this case, the relative concentration of such "traps" varied within the limits of 10^{-5} to 10^{-3} at^{-1}. As the initial H concentration, we considered the corresponding value of the steady-state solution (5) $C_\mathrm{H}(x)$, at a depth of $x = 1$ μm.

At the first stage of H_n nucleation, we assume that hydrogen is captured at "traps," forming T–H ("trap"–hydrogen) complexes. At this stage, the growth of such a complex was traced using the following system of equations:

$$\frac{dC_\mathrm{TH}}{dt} = R^+_\mathrm{TH} - R^-_\mathrm{TH} - R^+_\mathrm{TH2} + R^-_\mathrm{TH2},$$

$$R^+_\mathrm{TH} = Z_\mathrm{H} Z_\mathrm{T} \nu C_\mathrm{H} C_\mathrm{T}; \quad R^-_\mathrm{TH} = \nu C_\mathrm{TH} \exp\left(-\frac{E_\mathrm{b}}{kT}\right),$$

$$R^+_\mathrm{TH2} = Z_\mathrm{H} Z_\mathrm{TH} \nu C_\mathrm{H} C_\mathrm{TH}; \quad R^-_\mathrm{TH2} = \nu C_\mathrm{HT2} \exp\left(-\frac{E_\mathrm{b}}{kT}\right),$$

where C_T is the initial concentration of "traps;" C_TH, C_TH2 are the concentrations of T–H complexes (containing 1 and 2 atoms, respectively); R^+_TH, R^-_TH are the rates of the formation and decay of T–H complexes; R^+_TH2, R^-_TH2 are the rates of the formation and decay of T–H2 complexes containing 2 hydrogen atoms; Z_H, Z_T are the geometric factors, which are dependent on the "trap" forms; ν is the hydrogen mobility; and E_b is the hydrogen–"trap" binding energy. The growth of clusters containing n hydrogen atoms for $n \le 8$ is described similarly:

$$\frac{dC_{\mathrm{TH}n}}{dt} = R^+_{\mathrm{TH}n} - R^-_{\mathrm{TH}n} - R^+_{\mathrm{TH}n+1} + R^-_{\mathrm{TH}n+1},$$

$$R^+_{\mathrm{TH}n} = Z_\mathrm{H} Z_{\mathrm{TH}n-1} \nu C_\mathrm{H} C_{\mathrm{TH}n-1};$$

$$R^-_{\mathrm{TH}n} = \nu C_{\mathrm{HT}n} \exp\left(-\frac{E_\mathrm{b}}{kT}\right),$$

$$R^+_{\mathrm{TH}n+1} = Z_\mathrm{H} Z_{\mathrm{TH}n} \nu C_\mathrm{H} C_{\mathrm{TH}n};$$

$$R^-_{\mathrm{TH}n+1} = \nu C_{\mathrm{HT}n+1} \exp\left(-\frac{E_\mathrm{b}}{kT}\right),$$

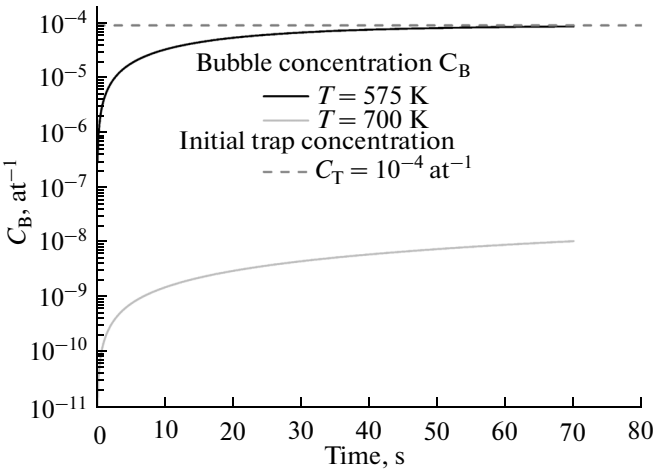

Fig. 1. Time evolution of the concentration of stable hydrogen bubbles (C_B) for two temperature values (T = 575 and 700 K), a fixed initial "trap" concentration of $C_T = 10^{-4}$ at^{-1}, and an implanted hydrogen atom flux of $F_H = 10^{22}$ m^{-2} s^{-1}.

where C_{THn}, C_{THn-1}, C_{THn+1} are the concentrations of T–H complexes containing n, $n-1$, $n+1$ hydrogen atoms, respectively, and R^+_{THn}, R^-_{THn}, R^+_{THn+1}, R^-_{THn+1} are the rates of the formation and decay of T–H complexes containing n and $n+1$ hydrogen atoms.

From the results of quantum-mechanical calculations [21], the binding energy of H atoms with "traps" was assumed to be 0.5 eV. Moreover, as shown in [21], the binding energy of hydrogen with a dislocation changes insignificantly in the range $n \le 8$ (i.e., up to 8 atoms in a cluster); therefore, in our calculations, we assumed that the binding energy is constant. The hydrogen mobility was calculated using the relation $\nu = D/a_0^2$, where a_0 is the W lattice constant ($a_0 = 3.14$ Å).

The second stage of cluster growth was considered after the number of H atoms captured at the "trap" reached the critical value (equal to 8). In this case, the bubble-growth mechanism was due to the emission of interstitial atoms with the formation of dislocation jogs. We note that, the effectiveness of HI capture in the presence of a dislocation jog turns out to be significantly stronger than in the above case of traps in the "ideal" dislocation core and is comparable in magnitude with that of H-atom capture at a single vacancy. In this case, the binding energy is on the order of several electronvolts [25–28]. Therefore, we assumed at this stage that the "trap" transforms into a stable bubble-nucleation center with a binding energy of 2 eV [21]. Because we considered only the initial stage of bubble formation, the possible dependence of the binding energy on the bubble size was not taken into account. The concentration of such unsaturated "traps" was traced using the following equations:

$$\frac{dC_B}{dt} = R^+_B - R^-_B,$$

$$R^+_B = Z_H Z_{NH7} \nu C_H C_{NH7}, \quad R^-_B = \nu C_B \exp\left(-\frac{E_b}{kT}\right),$$

where C_B is the concentration of unsaturated "traps" (i.e., bubbles); R^+_B, R^-_B are the rates of bubble growth and decay, respectively; and C_{NH7} is the concentration of complexes containing seven H atoms.

After the formation of a stable nucleation center, further growth of the bubble and its size (i.e., the number of held H atoms) were traced using the following equations:

$$\frac{dN_{HB}}{dt} = R^+_{NHB} - R^-_{NHB},$$

$$R^+_{NHB} = Z_H Z_B \nu C_H C_B; \quad R^-_{NHB} = \nu C_B \exp\left(-\frac{E_b}{kT}\right),$$

where N_{HB} is the bubble size (the number of H atoms) and R^+_{NHB}, R^-_{NHB} are the rates of H-atom arrival and evaporation. In all the above relations, all geometric factors were assumed to be unity ($Z = 1$).

RESULTS AND DISCUSSION

Figure 1 shows the time evolution of the concentration of stable hydrogen bubbles (C_B) in W for two different temperatures (575 and 700 K) and fixed values of the "trap" concentration ($C_T = 10^{-4}$ at^{-1}) and the hydrogen atom flux ($F_H = 10^{22}$ m^{-2} s^{-1}). As is seen from the figure, the concentration of stable bubbles (C_B) at a temperature of $T = 575$ K reaches that of the initial "traps" C_T during a period of time of $t \sim 50$ s. This means that the states of almost all initial "traps" transform into those of stable bubbles. At the same time, at a higher temperature of $T = 700$ K, only small portion of "traps" became stable bubbles ($C_B \ll C_T$). This can be explained by the fact that, as the temperature increases, the rate of T–H-complex decay increases and significantly exceeds that of hydrogen capture at "traps." It can be assumed that, as the temperature increases (above a certain "threshold" value), a considerable number of clusters H_n formed at "traps" do not reach the "critical" size ($n = 8$); and therefore, the mechanism of their further growth because of the emission of interstitials in this case does not work. Thus, it is seen that, under the given bombardment conditions and the material structure, the temperature significantly affects the effectiveness of the formation and growth of hydrogen bubbles on dislocations (because of the mechanism of emission of interstitial atoms) and, as a consequence, affects the probability of bubble and blister formation.

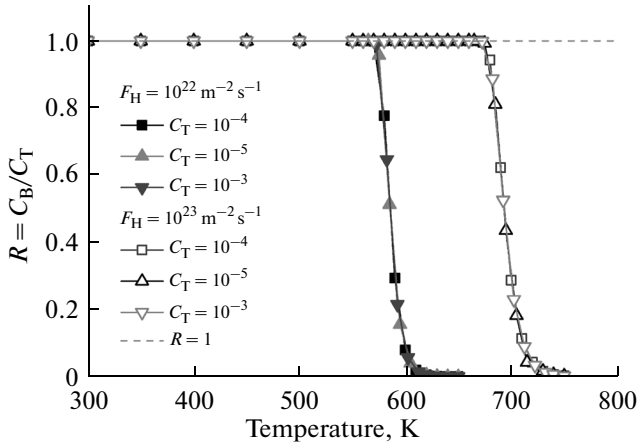

Fig. 2. Temperature dependence of the relative concentration of stable hydrogen bubbles R for different trap concentrations of $C_T = 10^{-3}$, 10^{-4}, and 10^{-5} at^{-1} and two implanted hydrogen fluxes of $F_H = 10^{22}$ and 10^{23} m^{-2} s^{-1}.

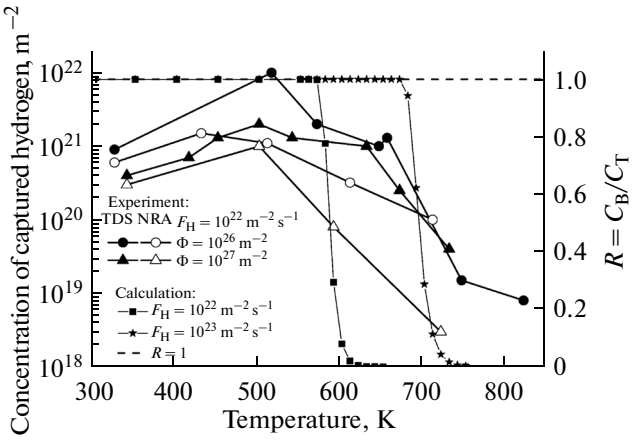

Fig. 3. Comparison of the calculated temperature dependence of the relative concentration of stable hydrogen bubbles R for different implantation fluxes F_H with the experimental data in [8], which describe the temperature dependence of the captured H concentration in W for different total fluences Φ of implanted hydrogen. The experimental data were obtained using nuclear reaction analysis (NRA) and thermal desorption spectroscopy (TDS). The experimental concentration of captured hydrogen in W is given on the left vertical scale. The calculated ratio ($R = C_B/C_T$) of the concentration of stable hydrogen bubbles to the initial concentration of "traps" is given on the right vertical scale.

Figure 2 shows the temperature dependence of the relative concentration of stable bubbles R (where $R = C_B/C_T$) for different values of the initial "trap" concentration C_T and the implantation hydrogen flux F_H. It can be seen from this figure that, for a fixed implantation flux, varying the initial "trap" concentration barely affects the dynamics of the formation and growth of stable hydrogen bubbles. This is related to the fact that the rate of hydrogen arrival at "traps" is proportional to their concentration. Thus, varying the initial "trap" concentration, we thereby vary the rate of arrival of hydrogen atoms at them; in this case, the dynamics of "trap" filling with HI atoms in relative units does not change.

Figure 3 shows the qualitative comparison of the temperature dependence of the relative concentration of hydrogen captured at "traps," which was obtained using calculations with corresponding experimental data [8]. The experimental concentration of captured hydrogen in W is given on the left vertical scale. The four shown curves correspond to the data obtained for two values of the gathered total fluence (10^{26} and 10^{27} m^{-2}) using two different methods: nuclear reaction analysis (NRA) and thermal desorption spectroscopy (TDS). The calculated ratio of the concentration of stable hydrogen bubbles to the initial concentration of "traps" $R = C_B/C_T$ (for times on the order of 70 s corresponding to steady-state formation) is read from the right vertical scale. The ratio $R = 1$ indicate that states of all "traps" transform into stable hydrogen bubbles, which continue to grow because of the emission of interstitial atoms. As can be seen from this figure, for a fixed flux, a certain threshold temperature at which R decreases sharply exists. For flux values in the range of 10^{22}–10^{23} m^{-2} s^{-1}, the threshold temperature is 600–700 K, respectively. It is important to note that the threshold temperature also increases with increasing flux F_H. This can be explained by a change in the balance between the rates of capture and loss of hydrogen atoms at the growing bubble: as the flux increases (and, as a consequence, as the rate of H capture at clusters increases), a higher rate of T–H complex decay (i.e., a higher temperature) is required to decrease the effectiveness of the bubble growth on "traps."

The obtained values of the threshold temperature agree qualitatively with the experimental data [8], according to which a significant decrease in the amount of hydrogen retained in W is observed at a temperature of about 600 K (Fig. 3). In addition, the fact that, in accordance with the experimental data in [7], the formation of hydrogen bubbles and blisters was not observed in bombarded W at temperatures above 700 K is evidence in favor of the proposed model. The attained qualitative agreement with the experimental data allows us to conclude that our considered mechanism for hydrogen-bubble formation and growth at dislocations can play an important role in the retention and accumulation of hydrogen isotopes under bombardment with low-energy plasma fluxes in the "subthreshold" mode, in which stable defects of the W crystal lattice do not form.

CONCLUSIONS

We have analyzed mechanisms for hydrogen capture in W under conditions of the "subthreshold" implantation mode (in which primary structural

defects do not form); they are due to hydrogen-bubble growth at dislocations. Using numerical simulation, which was carried out within the framework of kinetic theory using the results of quantum-mechanical ab-initio calculations, we analyzed bombardment conditions corresponding to the formation of "above-critical" clusters H_n (which were nucleation centers of hydrogen bubbles, the further growth of which was due to a mechanism for the emission of interstitial atoms and due to the formation of dislocation jogs). We showed that not only the temperature, but also the plasma flux intensity affect the hydrogen-bubble-formation process. The obtained values of the threshold temperature (at which bubble growth decreases sharply) agree with the existing experimental data, which explicitly indicate a significant decrease in the total amount of retained hydrogen in W at temperatures above 500 K and the absence of blisters and bubbles at $T > 700$ K. To improve quantitative agreement of the calculated results with the experimental data, further development of the model and the extension of the set of microscopic parameters describing bubble-growth processes inside polycrystalline material grains and at their boundaries are required.

REFERENCES

1. R. E. Clark and D. Reiter, *Nuclear Fusion Research: Understanding Plasma-Surface Interactions* (Springer, Berlin, 2005).
2. G. Pintsuk, Compr. Nucl. Mater. **4**, 551 (2012).
3. Y. Zayachuk, M. H. J. 't Hoen, P. A. Zeijlmans van Emmichoven, D. Terentyev, I. Uytdenhouwen, and G. van Oost, Nucl. Fusion **53**, 013013 (2013).
4. Y. Zayachuk, M. H. J. 't Hoen, P. A. Zeijlmans van Emmichoven, D. Terentyev, I. Uytdenhouwen, and G. van Oost, Nucl. Fusion **52**, 103021 (2012).
5. K. Schmid, V. Rieger, and A. Manhard, J. Nucl. Mater. **426**, 247 (2012).
6. K. O. E. Henriksson, K. Nordlund, A. Krasheninnikov, and J. Keinonen, Appl. Phys. Lett. **87**, 163113 (2005).
7. J. Roth and K. Schmid, Phys. Scr. T **2011**, 014031 (2011).
8. V. Kh. Alimov, B. Tyburska-Püschel, S. Lindig, Y. Hatano, M. Balden, J. Roth, K. Isobe, M. Matsuyama, and T. Yamanishi, J. Nucl. Mater. **420**, 519 (2012).
9. O. V. Ogorodnikova, J. Roth, and M. Mayer, J. Nucl. Mater. **313–316**, 469 (2003).
10. A. van Veen, H. A. Filius, J. de Vries, K. R. Bijkerk, G. J. Rozing, and D. Segers, J. Nucl. Mater. **155–157**, 1113 (1988).
11. K. Nordlund, C. Bjorkas, T. Ahlgren, and A. A. E. Sand, J. Phys. D: Appl. Phys. **47**, 224018 (2014).
12. G.-H. Lu, H.-B. Zhou, and C. S. Becquart, Nucl. Fusion **54**, 086001 (2014).
13. E. A. Denisov, T. N. Kompaniets, A. A. Kurdyumov, S. N. Mazayev, and Yu. G. Prokofiev, J. Nucl. Mater. B **212–215**, 1448 (1994).
14. E. Denisov, T. Kompaniets, A. Kurdyumov, and S. Mazayev, J. Nucl. Mater. **233–237**, 1218 (1996).
15. E. A. Denisov and T. A. Kompaniets, Tech. Phys. **46**, 240 (2001).
16. V. N. Lobko and I. N. Bekman, Al'tern. Energet. Ekol. **10** (90), 36 (2010).
17. V. N. Lobko and I. N. Bekman, Al'tern. Energet. Ekol. **11** (91), 38 (2010).
18. V. N. Lobko and I. N. Bekman, Al'tern. Energet. Ekol. **4** (96), 20 (2011).
19. T. Ahlgren, K. Heinola, and J. Keinonen, J. Nucl. Mater. **427**, 152 (2012).
20. P. Yu. Grigorev, V. I. Dubinko, D. A. Terentyev, A. V. Bakaev, and E. E. Zhurkin, J. Surf. Invest.: X-ray, Synchrotron Neutron Tech. **8**, 234 (2014).
21. D. Terentyev, V. Dubinko, A. Bakaev, Y. Zayachuk, W. van Renterghem, and P. Grigorev, Nucl. Fusion **54**, 042004 (2014).
22. R. Frauenfelder, J. Vacuum Sci. Technol. **6**, 388 (1969).
23. G. S. Was, *Fundamentals of Radiation Materials Science: Metals and Alloys* (Springer, Berlin, New York, 2007).
24. D. Hull and D. J. Bacon, *Introduction to Dislocations*, 4th ed. (Butterworth-Heinemann, Linacre House, Oxford, 2001).
25. V. I. Dubinko, S. Hu, Y. Li, C. H. Henager, and R. J. Kurtz, Philos. Mag. **92**, 4113 (2012).
26. D. F. Johnson and E. A. Carter, J. Mater. Res. **25**, 315 (2010).
27. X. S. Kong, Y. You, Q. F. Fang, C. S. Liu, J.-L. Chen, G.-N. Luo, B. C. Pan, and Z. Wanget, J. Nucl. Mater. **433**, 357 (2013).
28. K. Heitola, T. Ahlgren, K. Nordlund, and J. Keinonen, Phys. Rev. B **82**, 094102 (2010).

Translation by L. Kulman